Preference of H2 as Hydrogen Source in Hydrogenation of Ketones Catalyzed by Late Transition Metal Complexes. A DFT Study

ARTICLE *in* ORGANOMETALLICS · JANUARY 2010

Impact Factor: 4.13 · DOI: 10.1021/om900434n

4 AUTHORS, INCLUDING:

Ming Lei
Beijing University of Chemical Technology
58 PUBLICATIONS **437** CITATIONS

ORGANOMETALLICS
Article

Organometallics **2010,** *29,* 543–548 543
DOI: 10.1021/om900434n

Preference of H_2 as Hydrogen Source in Hydrogenation of Ketones Catalyzed by Late Transition Metal Complexes. A DFT Study

Ming Lei,*,† Wenchao Zhang,† Yue Chen,† and Yanhui Tang‡

†*State Key Laboratory of Chemical Resource Engineering, Institute of Materia Medica, College of Science, Beijing University of Chemical Technology, Beijing 100029, People's Republic of China* and ‡*School of Materials Science & Engineering, Beijing Institute of Fashion Technology, Beijing 100029, People's Republic of China*

Received May 24, 2009

In this work, H_2 activation processes in hydrogenation of ketones catalyzed by late transition metal−ligand bifunctional catalysts have been studied using the DFT method. For systems A (RuH_2-diphosephine/diamine complex) and B (Ru-η^5-Cp*-1,2-diamine complex), the dihydrogen activation process in neutral and basic conditions (path 1) consisted of two steps: H_2 coordination and H−H cleavage. However, dihydrogen activations catalyzed by complexes C−F (Ru-η^6-arene and Rh/Ir-cyclopentadiene complexes) along path 1 consist of only H−H cleavage due to the absence of H_2 coordination. Thus, systems C−F have higher energy barriers ($\Delta G > 27$ kcal/mol) for dihydrogen activation than systems A and B. However, for systems C−F under acidic conditions, dihydrogen activation (path 2) consists of the two steps involving H_2 coordination; thus the dihydrogen activation barriers decrease greatly, resulting in an easy splitting of H_2. These results agree well with experiments. In the conversion from transfer hydrogenation to H_2 hydrogenation for C−F, the protonation of 16*e* complex MN_{C-F} changes the $N^2-M^1-Y^3$ (Y = N or O) delocalized π-bond into a M^1-Y^3 localized π-bond. Therefore, the 16*e* complexes, which can provide a vacant site for H_2 coordination, tend to perform H_2 hydrogenation.

Introduction

Asymmetric hydrogenation of ketone is one of the most important and widely used synthetic methods to produce chiral alcohols. Currently, two synthetic methods were developed for the homogeneous enantioselective ketone hydrogenation according to the use of hydrogen sources: one of them, H_2 hydrogenation (HH), utilizes molecular dihydrogen, while the other, transfer hydrogenation (TH), uses organic hydrogen sources (alcohols or formic acid).[1−7] Late transition metal−diamine systems appear to be the most efficient catalysts in both approaches. One of the most efficient HH catalysts is the combination of a ruthenium metal center bearing a chiral bisphosphine and a chiral diamine ligand developed by Noyori et al. (RuH_2-diphosephine/diamine, Scheme 1a, A).[8−14] Ikariya et al. reported another quite efficient HH catalyst, RuCp*-1,2-diamnie complex (Cp* = η^5-C_5-$(CH_3)_5$ (Scheme 1a, B), which does not have a phosphine ligand.[3,12,15] In the mid-1990s, Noyori and co-workers synthesized η^6-arene-Ru complexes bearing monotosylated 1,2-diamine (Scheme 1a, C) or amino alcohols (Scheme 1a, D), which made a breakthrough of transition-metal-catalyzed transfer hydrogenation.[16−21] Rh/Ir-cyclopentadiene complexes with monotosylated 1,2-diamine

*Corresponding author. Phone: 86-10-6444-6598. Fax: 86-10-6444-6598. E-mail: leim@mail.buct.edu.cn.

(1) Noyori, R. *Angew. Chem., Int. Ed.* **2002**, *41*, 2008–2022.
(2) Clapham, S. E.; Hadzovic, A.; Morris, R. H. *Coord. Chem. Rev.* **2004**, *248*, 2201–2237.
(3) Ito, M.; Ikariya, T. *Chem. Commun.* **2007**, 5134–5142.
(4) Samec, J. S. M.; Backvall, J. E.; Andersson, P. G.; Brandt, P. *Chem. Soc. Rev.* **2006**, *35*, 237–248.
(5) Palmer, M. J.; Wills, M. *Tetrahedron: Asymmetry* **1999**, *10*, 2045–2061.
(6) Wang, C.; Wu, X.; Xiao, J. *Chem. Asian J.* **2008**, *3*, 1750–1770.
(7) Ikariya, T.; Blacker, A. J. *Acc. Chem. Res.* **2007**, *40*, 1300–1308.
(8) Ohkuma, T.; Ooka, H.; Hashiguchi, S.; Ikariya, T.; Noyori, R. *J. Am. Chem. Soc.* **1995**, *117*, 2675–2676.
(9) Sandoval, C. A.; Ohkuma, T.; Muniz, K.; Noyori, R. *J. Am. Chem. Soc.* **2003**, *125*, 13490–13503.
(10) Abdur-Rashid, K.; Clapham, S. E.; Hadzovic, A.; Harvey, J. N.; Lough, A. J.; Morris, R. H. *J. Am. Chem. Soc.* **2002**, *124*, 15104–15118.
(11) Chen, Y.; Liu, S.; Lei, M. *J. Phys. Chem. C* **2008**, *112*, 13524–13527.
(12) Hedberg, C.; Kallstrom, K.; Arvidsson, P. I.; Brandt, P.; Andersson, P. G. *J. Am. Chem. Soc.* **2005**, *127*, 15083–15090.
(13) Di Tommaso, D.; French, S. A.; Zanotti-Gerosa, A.; Hancock, F.; Palin, E. J.; Catlow, C. R. A. *Inorg. Chem.* **2008**, *47*, 2674–2687. Di Tommaso, D.; French, S. A.; Catlow, C. R. A. *J. Mol. Struct.: THEOCHEM* **2007**, *812*, 39–49.
(14) Chen, Y.; Tang, Y.; Lei, M. *Dalton Trans* **2009**, *13*, 2359–2364.
(15) Ito, M.; Hirakawa, M.; Murata, K.; Ikariya, T. *Organometallics* **2001**, *20*, 379–381.
(16) Hashiguchi, S.; Fujii, A.; Takehara, J.; Ikariya, T.; Noyori, R. *J. Am. Chem. Soc.* **1995**, *117*, 7562–7563. Fujii, A.; Hashiguchi, S.; Uematsu, N.; Ikariya, T.; Noyori, R. *J. Am. Chem. Soc.* **1996**, *118*, 2521–2522.
(17) Yamakawa, M.; Ito, H.; Noyori, R. *J. Am. Chem. Soc.* **2000**, *122*, 1466–1478.
(18) Wu, X.; Liu, J.; Tommaso, D. D.; Iggo, J. A.; Catlow, C. R. A.; Bacsa, J.; Xiao, J. *Chem.—Eur. J.* **2008**, *14*, 7699–7715.
(19) Alonso, D. A.; Brandt, P.; Nordin, S.; Andersson, P. G. *J. Am. Chem. Soc.* **1999**, *121*, 9580–9588.
(20) Noyori, R.; Yamakawa, M.; Hashiguchi, S. *J. Org. Chem.* **2001**, *66*, 7931–7944.
(21) Pannetier, N.; Sortais, J.-B.; Dieng, P. S.; Barloy, L.; Sirlin, C.; Pfeffer, M. *Organometallics* **2008**, *27*, 5852–5859.

Published on Web 01/08/2010

Scheme 1. (a) Typical TM Catalysts Used in Hydrogenation of Ketones; (b) Mechanisms of H_2 Activation under Various Conditions

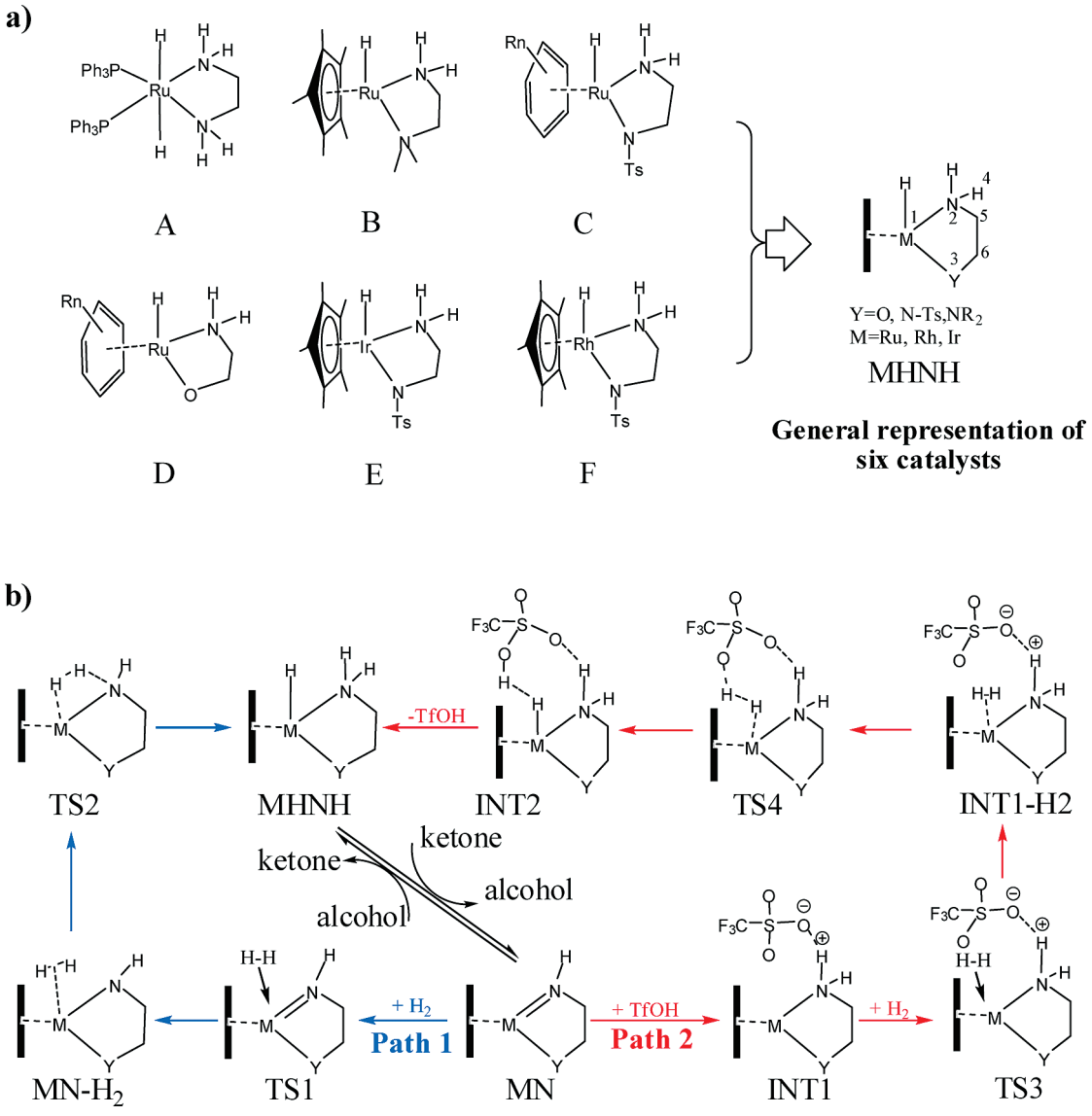

ligands (Scheme 1a, E and F) also show good activity in TH, which are analogous with complex C.[7,22−26] Although all listed catalysts above contain an M−H/N−H functional framework (where M = Ru, Rh, or Ir; we abbreviate these complexes as MHNH, shown in Scheme 1a), their activities differ greatly. It was demonstrated that catalysts A and B are efficient for HH, while systems C−F are typically used for TH. Some Ru(II) diphosphine/diamine complexes could hydrogenate acetophenone using both 2-propanol and H_2, but the reaction rates for TH are lower than those for HH.[27−29] On the contrary, catalysts C−F can easily catalyze TH but difficultly carry out HH. Dahlenburg et al. found a hydridoiridium complex, which is similar to a Ru-diphosphine/diamine complex in structure, which favored TH over HH, and attributed this preference to the inability of H_2 to displace a coordinated solvent molecule from an intermediate hydrido complex.[30] Recently, complexes C and E were reported to be good catalysts for HH reaction in acidic conditions.[3,6,31−35] Our previous work found that the acidic molecule could

(22) Murata, K.; Ikariya, T.; Noyori, R. *J. Org. Chem.* **1999**, *64*, 2186–2187.
(23) Matharu, D. S.; Morris, D. J.; Clarkson, G. J.; Wills, M. *Chem. Commun.* **2006**, *30*, 3232–3234.
(24) Wu, X.; Li, X.; Zanotti-Gerosa, A.; Pettman, A.; Liu, J.; Mills, A. J.; Xiao, J. *Chem.—Eur. J.* **2008**, *14*, 2209–2222.
(25) Heiden, Z. M.; Rauchfuss, T. B. *J. Am. Chem. Soc.* **2009**, *131*, 3593–3600.
(26) Shirai, S.-y.; Nara, H.; Kayaki, Y.; Ikariya, T. *Organometallics* **2009**, *28*, 802–809.
(27) Lindner, E.; Mayer, H. A.; Warad, I.; Eichele, K. *J. Org. Chem.* **2003**, *665*, 176–185.
(28) Ma, G.; McDonald, R.; Ferguson, M.; Cavell, R. G.; Patrick, B. O.; James, B. R.; Hu, T. Q. *Organometallics* **2007**, *26*, 846–854.
(29) Xia, Y.-Q.; Tang, Y.-Y.; Liang, Z.-M.; Yu, C.-B.; Zhou, X.-G.; Li, R.-X.; Li, X.-J. *J. Mol. Catal. A: Chem.* **2005**, *240*, 132–138.
(30) Dahlenburg, L.; Götz, R. *Inorg. Chim. Acta* **2004**, *357*, 2875–2880. Puchta, R.; Dahlenburg, L.; Clark, T. *Chem.—Eur. J.* **2008**, *14*, 8898–8903. Dahlenburg, L.; Menzel, R.; Heinemann, F. W. *Eur. J. Inorg. Chem.* **2007**, *2007*, 4364–4374.
(31) Ohkuma, T.; Utsumi, N.; Tsutsumi, K.; Murata, K.; Sandoval, C.; Noyori, R. *J. Am. Chem. Soc.* **2006**, *128*, 8724–8725.
(32) Sandoval, C. A.; Ohkuma, T.; Utsumi, N.; Tsutsumi, K.; Murata, K.; Noyori, R. *Chem. Asian J.* **2006**, *1*, 102–110.
(33) Ohkuma, T.; Tsutsumi, K.; Utsumi, N.; Arai, N.; Noyori, R.; Murata, K. *Org. Lett.* **2007**, *9*, 255–257.
(34) Ohkuma, T.; Utsumi, N.; Watanabe, M.; Tsutsumi, K.; Arai, N.; Murata, K. *Org. Lett.* **2007**, *9*, 2565–2567.
(35) Chen, Y.; Tang, Y.; Liu, S.; Lei, M.; Fang, W. *Organometallics* **2009**, *28*, 2078–2084.

participate in the H_2 activation process of HH catalyzed by C in acidic conditions.[35] However, the reasons for the observed preference for hydrogen sources of these transition metal (TM) catalysts with different structural frameworks in ketone hydrogenation are still unclear.[2,6,15]

The proposed mechanisms of HH and TH are shown in Scheme 1b. It is expected that HH and TH reactions are both initiated by transferring hydrogen from MHNH to ketones to generate alcohol and 16-electron complex MN via a metal−ligand bifunctional mechanism.[9,12,15,17,20,36] The next step is the production of MHNH from MN. There is an intrinsic difference in this step between HH and TH. For TH, MN regenerates starting MHNH complex by dehydrogenating alcohol or formic acid to complete the catalytic cycle. For HH, however, production of MHNH from MN is achieved by activation of H_2 under various conditions. In basic and neutral conditions (path 1 in Scheme 1b), in the first step, H_2 coordinates with MN and forms a η^2-H_2 complex ($MN-H_2$). This process proceeds via a transition state TS1. Then, heterolytic H−H bond cleavage, occurring via a four-membered transition state TS2, results in regeneration of MHNH.[10−12,14,35] In acidic conditions (path 2 in Scheme 1b), MN can get a proton from acid CF_3SO_3H, which was used in experiments (abbreviated as TfOH) to produce a protonated intermediate INT1, which is an ion pair of TfO^- and MNH^+, followed by H_2 coordination to form a η^2-H_2 intermediate (INT1-H_2) via transition state TS3.[31,32,35] Then, H_2 cleaves via transition state TS4 assisted by counteranion TfO^-, forming an adduct (INT2) of MHNH and TfOH. As a result, it could regenerate MHNH with the dissociation of a TfOH from INT2.[35] In acidic conditions, the alcohol solvent is expected to be important for the proton relay. Our previous study found TfOH and alcohol could participate in H_2 activation catalyzed by C together. The reaction proceeds similarly to path 2, and the alcohol acts as media to transfer proton with a little higher barrier compared with path 2.[35] It should be noted that the use of alcoholic solvents is crucial for catalytic efficiency. The presence of TfOH is important; the involvement of alcohol is also very important. However, H_2 activations assisted directly by TfO^- or alcohol and that assisted by TfOH and alcohol together have a common feature: H_2 coordination with the 16*e* TM complex in acidic conditions.

In this paper, we elucidate the differences in dihydrogen activation by these six (A−F) systems at the DFT level. Our results indicate that in HH dihydrogen can coordinate with the 16*e* complexes (MN_{A-B} and $INT1_{C-F}$), forming η^2-H_2 intermediates, but in TH, the dihydrogen activation process does not involve η^2-H_2 intermediates, resulting in a higher barrier (especially the free energy barrier). The ability of the 16*e* TM complexes to accept H_2 coordination is strongly related to the preference of dihydrogen sources used in hydrogenation of ketones in nature.

Computational Details

Geometries of transition states, intermediates, and separated reactants were optimized using the Gaussian03 program package[37] at density functional theory (DFT) level by means of the hybrid B3LYP functional[38,39] without any geometric constraints. The LANL2DZ[40] basis set was used for TM atoms and 6-31+G** for other atoms. We denote this calculation level as B3LYP/BSI. The existence of only one imaginary frequency for each transition state was confirmed by analytical frequency calculations. In these calculations the PPh_3, η^6-arene, and Cp* ligands of the complexes were simplified to PH_3, benzene, and cyclopentadienyl, respectively. Tosyl groups in C, E, and F were replaced by mesyl groups. Solvent effects (methanol and benzene) were evaluated using the polarizable continuum model (PCM).[41] Due to common structural M−H/N−H of these six complexes, we use $MHNH_X$ and MN_X (X = A−F) notations to describe the original complexes and their corresponding 16-electron derivatives, respectively.

Results and Discussion

The atomic labels of catalysts are shown in MHNH in Scheme 1. Along path 1, MN is the key complex to activate dihydrogen to regenerate complex MHNH. In MN_A and MN_B, the calculated M^1-N^2 bond lengths (2.011 and 1.952 Å) are much shorter than those in $MHNH_A$ and $MHNH_B$ (2.217 and 2.213 Å). Sums of bond angles (SA_{N2} = $\angle M^1-N^2-H^4 + \angle H^4-N^2-C^5 + \angle C^5-N^2-M^1$) around N^2 are 352.7° and 359.8°, respectively (Figure S1 in Supporting Information). These indicate that N^2 is an sp^2-N center, and its lone pair is involved in the formation of a π-bond with the M atom.[10,42−44] In MN_C, MN_E, and MN_F, the (a) M^1-N^2 bond lengths are 1.924, 1.917, and 1.921 Å; (b) SA_{N2} are 359.2°, 359.2°, and 359.0°; (c) M^1-N^3 bond lengths are 2.092, 2.055, and 2.081 Å, and (d) sums of bond angles (SA_{N3} = $\angle M^1-N^3-S^7 + \angle S^7-N^3-C^6 + \angle C^6-N^3-M^1$, S^7 is the sulfur atom in mesyl group) around N^3 are 351.9°, 351.1°, and 347.3°, respectively. These indicate that N^2 and N^3 are both sp^2-N centers and there are delocalized π-bonds in the $N^2-M^1-N^3$ moiety of MN_X (where X = C, E, and F).[45] Even for MN_D, where N^3 is replaced by oxygen, such a delocalized π-bond still exists.

For complexes A and B, H_2 activation in basic and neutral conditions can take place via path 1. Coordination of H_2 to

(36) Hadzovic, A.; Song, D.; MacLaughlin, C. M.; Morris, R. H. *Organometallics* **2007**, *26*, 5987–5999.
(37) Frisch, M. J.; Trucks, G. W.; Schlegel, H. B.; Scuseria, G. E.; Robb, M. A.; Cheeseman, J. R.; Montgomery, J. A., Jr.; Vreven, T.; Kudin, K. N.; Burant, J. C.; Millam, J. M.; Iyengar, S. S.; Tomasi, J.; Barone, V.; Mennucci, B.; Cossi, M.; Scalmani, G.; Rega, N.; Petersson, G. A.; Nakatsuji, H.; Hada, M.; Ehara, M.; Toyota, K.; Fukuda, R.; Hasegawa, J.; Ishida, M.; Nakajima, T.; Honda, Y.; Kitao, O.; Nakai, H.; Klene, M.; Li, X.; Knox, J. E.; Hratchian, H. P.; Cross, J. B.; Bakken, V.; Adamo, C.; Jaramillo, J.; Gomperts, R.; Stratmann, R. E.; Yazyev, O.; Austin, A. J.; Cammi, R.; Pomelli, C.; Ochterski, J. W.; Ayala, P. Y.; Morokuma, K.; Voth, G. A.; Salvador, P.; Dannenberg, J. J.; Zakrzewski, V. G.; Dapprich, S.; Daniels, A. D.; Strain, M. C.; Farkas, O.; Malick, D. K.; Rabuck, A. D.; Raghavachari, K.; Foresman, J. B.; Ortiz, J. V.; Cui, Q.; Baboul, A. G.; Clifford, S.; Cioslowski, J.; Stefanov, B. B.; Liu, G.; Liashenko, A.; Piskorz, P.; Komaromi, I.; Martin, R. L.; Fox, D. J.; Keith, T.; Al-Laham, M. A.; Peng, C. Y.; Nanayakkara, A.; Challacombe, M.; Gill, P. M. W.; Johnson, B.; Chen, W.; Wong, M. W.; Gonzalez, C.; Pople, J. A. *Gaussian03*; Gaussian, Inc.: Wallingford CT, 2004.
(38) Becke, A. D. *J. Chem. Phys.* **1993**, *98*, 5648–5652.
(39) Lee, C.; Yang, W.; Parr, R. G. *Phys. Rev. B* **1988**, *37*, 785–789.
(40) Hay, P. J.; Wadt, W. R. *J. Chem. Phys.* **1985**, *82*, 299.
(41) Barone, V.; Cossi, M. *J. Phys. Chem. A* **1998**, *102*, 1995–2001. Cossi, M.; Rega, N.; Scalmani, G.; Barone, V. *J. Comput. Chem.* **2003**, *24* (6), 669–681.
(42) Breen, T. L.; Stephan, D. W. *Organometallics* **1996**, *15*, 4223–4227.
(43) Hey-Hawkins, E.; Lindenberg, F. *Organometallics* **1994**, *13*, 4643–4644.
(44) Vogeley, N. J.; Templeton, J. L. *Polyhedron* **2004**, *23*, 311–321.
(45) Albeniz, A. C.; Calle, V.; Espinet, P.; Gomez, S. *Inorg. Chem.* **2001**, *40*, 4211–4216.
(46) Ma, B.; Collins, C. L.; Schaefer, H. F. *J. Am. Chem. Soc.* **1996**, *118*, 870–879. Heinekey, D. M.; Oldham, W. J. *Chem. Rev.* **1993**, *93*, 913–926.

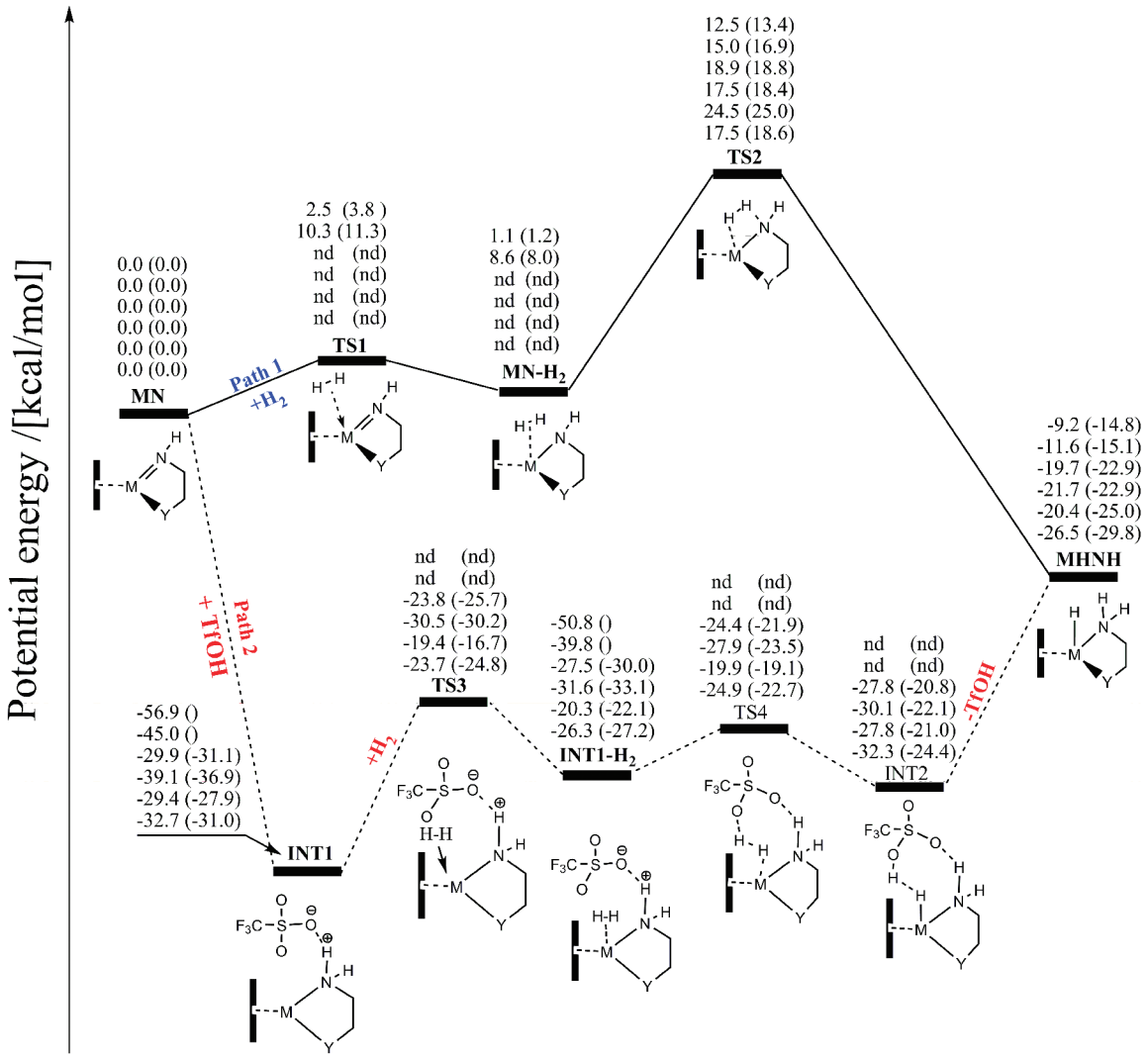

Figure 1. Energy profiles of dihydrogen activation. (Plain text is electronic energy and plain text in parentheses is the electronic energy with solvent effect of methanol; "nd" means the stationary point was not found; units: kcal/mol).

MN_X makes the M^1-N^2 bond lengths increase to 2.130 and 2.122 Å and SA_{N2} decrease to 329.6° and 328.2°, respectively. These findings imply that upon H_2 coordination N^2 has changed its character from sp^2 to sp^3 and the Ru^1-N^2 π-bond has been broken. In the next step, the H−H bond cleaves heterolytically and one hydrogen atom transfers to M^1 as a hydride, forming an M−H bond, and the other to N^2 as a proton, forming an N−H bond. The energy profile is shown in Figure 1 and Table 1. The calculated enthalpic barriers for H_2 coordination and H−H bond cleavage are 3.0 and 9.9 kcal/mol for A and 10.8 and 5.2 kcal/mol for B, respectively. The higher H_2 coordination barrier for B (relative to A) is due to the stronger Ru^1-N^2 π-bond in MN_B.

For catalysts C, D, E, and F, however, we were unable to locate the $MN-H_2$ intermediates; presumably the $MN-H_2$ interaction is weak and cannot produce a stable intermediate. This is consistent with the result calculated by Noyori et al. for C and D.[17] Attempts to optimize the artificial $MN-H_2$ structures finally led to parted MN and dihydrogen. As seen in Table 1, the calculated H−H bond cleavage barriers (relative to MN) for the C, D, E, and F systems (19.7, 18.4, 24.9, and 18.2 kcal/mol, respectively) are significantly larger than the barriers for A and B along path 1, and this reaction should take place with difficulty. In addition, the absence of H_2 coordination will lead to a great decrease of entropy and higher free energy barriers.[35] The free energy barriers for systems C−F are 28.6, 27.6, 34.2, and 27.5 kcal/mol, respectively, higher than that for systems A and B (Table 1).

As mentioned above, in acidic conditions the MN_X (where X = C, D, F, and E) complexes are in their protonated states, $INT1_X$. The protonated intermediates $INT1_X$ interact with H_2 and form η^2-H_2 complex $INT1_X-H_2$. Calculations show that protonation of MN_X occurs at the N^2 center; as a result, (a) the M^1-N^2 bond length increased by ca. 0.20 Å, (b) the M^1-N^3 bond length decreased about 0.12 Å, (c) SA_{N3} increased to about 358°, and (d) the N^2 center changed its character from sp^2 to sp^3. These findings imply that the delocalized $N^2-M^1-N^3$ π-bond has changed into a localized M^1-N^3 π-bond because of the protonation of MN_X. The H_2 activation by these protonated species is found to proceed also in two steps: H_2 coordination followed by H−H cleavage. Enthalpic barriers for H_2 coordination at TS3 (relative to $INT1_X$) calculated under vacuum are 7.0, 9.4, 10.8, and 9.5 kcal/mol, for X = C, D, E, and F, respectively. The next H−H heterolytic cleavage in $INT1_X-H_2$ proceeds with the

Table 1. Relative Energies Calculated at the B3LYP/BSI Level Including Potential Energy, Enthalpy, Free Energy, and Potential Energy with Solvent Effects (units: kcal/mol)

	MN	TS1	MN−H_2	TS2	INT1	TS3	INT1−H_2	TS4	INT2	MHNH
					Relative Enthalpy					
A	0.0	3.0	3.1	12.9	−53.1		−44.7			−4.7
B	0.0	10.8	10.6	15.8	−41.8		−34.2			−6.6
C	0.0			19.7	−27.0	−20.0	−22.0	−20.8	−21.6	−14.3
D	0.0			18.4	−35.9	−26.6	−26.3	−24.3	−24.0	−16.0
E	0.0			24.9	−26.4	−15.6	−15.6	−16.9	−21.5	−14.9
F	0.0			18.2	−29.6	−20.1	−21.2	−21.3	−25.9	−21.0
					Relative Free Energy					
A	0.0	10.4	11.0	22.0	−40.2		−25.3			3.7
B	0.0	19.3	19.4	25.4	−29.0		−15.5			2.1
C	0.0			28.6	−16.0	−0.1	−2.2	−0.1	−2.9	−5.7
D	0.0			27.6	−22.8	−6.5	−6.8	−4.0	−4.6	−7.4
E	0.0			34.2	−14.0	5.1	4.7	4.3	−1.6	−6.1
F	0.0			27.5	−17.4	−0.4	−0.4	0.0	−6.2	−12.1

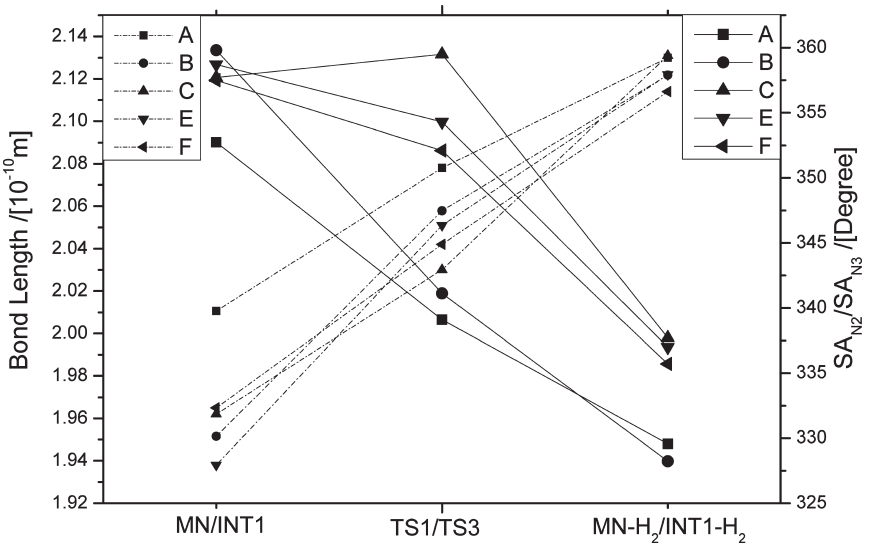

Figure 2. Structural changes in dihydrogen coordination with MN/INT1. Dotted line: M−N bond length; solid line: SA_N angle; for A and B, M−N and SA_N correspond to M^1−N^2 and SA_{N2}, and for C, E, and F, M−N and SA_N correspond to M^1−N^3 and SA_{N3}.

aid of TfO^-.[7] Enthalpic barriers of H−H cleavage are rather low (less than 2 kcal/mol). In experiments, there are rare reports about the hydrogenation of ketones catalyzed by A and B in acidic conditions. Herein, we also have studied the reaction along path 2 (in Scheme 1) catalyzed by A and B. TfOH interacts with MN_X (where X = A and B), forming very stable complex $INT1_X$ (enthalpies decreased 41.8 and 53.1 kcal/mol for A and B, respectively). $INT1_X$ can accept coordination of H_2 to produce η^2-H_2 complex $INT1_X$−H_2. However, the $INT2_X$ cannot be located and the optimization of artificially constructed $INT2_X$ finally led to $INT1_X$−H_2. In other words, the H−H cleavage step proceeds with difficulty for systems A and B in acid conditions. This is due to the higher hydridic property of H bonding with Ru in $MHNH_X$. The negative APT charges on the hydride in MHNH are −0.268, −0.230, −0.057, −0.120, −0.058, and −0.051 for A−F, respectively. It is notable that the hydrides in A and B carry more negative charge than those in C−F. Thus, the hydrides in A and B tend to interact with proton to generate a dihydrogen complex. $MHNH_A$ and $MHNH_B$ will react with strong acid TfOH to produce a η^2-H_2 complex, $INT1_A$−H_2 and $INT1_B$−H_2. A base or weak acid group is able to facilitate the dihydrogen splitting process for systems A and B. Then we use formic acid instead of TfOH to assist the cleavage of H_2 for systems A and B (see Supporting Information). Actually, in neural or slightly basic conditions, H_2 activation could occur via another pathway similar to path 2 proposed by Noyori et al., which competes with path 1.[9] The complex MN could get a proton from alcohol to be protonated, and the formed MNH^+ complex could accept H_2 coordination, forming a η^2-H_2 intermediate. The next H_2 cleavage is expected to proceed with the help of alcohols.

Solvent effect was also considered using the PCM method. Nonpolar benzene solvent has little influence on barriers of H_2 coordination (barriers vary less than 1.3 kcal/mol) and increases the barriers of H−H cleavage less than 2.3 kcal/mol (see Table S2 in Supporting Information). The solvent effect of methanol on the reaction is slightly larger than that of benzene. H_2 coordination has not been changed notably, but the barriers of H−H cleavage increase by 0.8, 2.6, 5.1, 5.9, 2.5, and 3.1 kcal/mol for A and B along path 1 and C−F along path 2, respectively. Because optimization of the intermediates and transition states using the CPCM method always encountered difficult convergence and additional

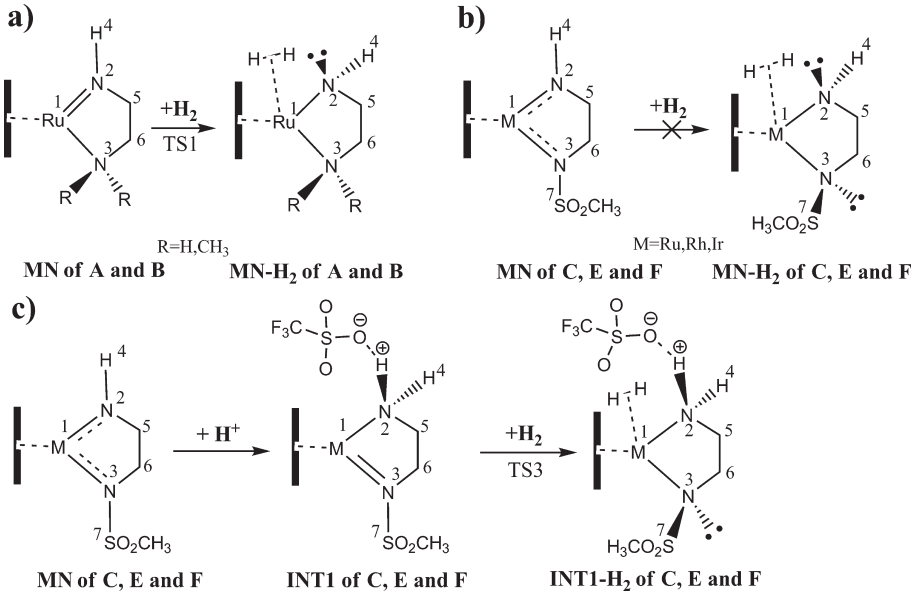

Figure 3. H_2 coordination with MN of (a) A and B in neutral conditions, (b) C, E, and F in neutral conditions, and (c) C, E, and F in acidic conditions.

imaginary frequencies, the results of optimization in solvent are not presented here.

Therefore the structural feature of 16*e* complexes is proposed to determine the occurrence of H_2 coordination. For A and B, the M^1-N^2 bond increases 0.119 and 0.170 Å and SA_{N2} decreases 23.2° and 31.6° in the H_2 coordination process, respectively. Similarly, the M^1-N^3 bond increases 0.168 Å and SA_{N3} decreases 21.2° for C, E, and F on average (Figure 2). In addition, M^1 atoms get more positive charge and N^2 atoms get more negative charge from MN (or INT1) to TS1 (or TS3). This indicates that the localized π-bond M^1-N^2 (or M^1-N^3) is broken in the H_2 coordination process and that the breaking of this π-bond provides the metal center with a vacant d-orbital to accept the H_2 coordination. The complexes MN_A and MN_B as well as $INT1_{C-F}$, which have a localized π-bond on M^1-N^2 or M^1-Y^3, could interact strongly with H_2, forming η^2-H_2 complexes (Figure 3a and c). In contrast, the 16*e* complexes MN_{C-F} all have a stronger delocalized $N^2-M^1-Y^3$ (for C, E, and F, Y = N atom; for D, Y = O atom) π-bond. It will cost much energy to break the delocalized π-bond for H_2 coordination, and the presumed $MN_{C-F}-H_2$ intermediates should be so unstable that we could not locate the η^2-H_2 complex $MN_{C-F}-H_2$ in neutral conditions (Figure 3b). The coordination of H_2 decreases the barrier of the whole dihydrogen activation despite A and B systems being under acidic conditions. Especially, the free energy barriers of dihydrogen activation are decreased sharply. Therefore, the coordination of H_2 is essential for the HH reaction.

Conclusion

In summary, the H_2 activation processes in the hydrogenation of ketones catalyzed by late transition metal−ligand bifunctional catalysts have been studied using the DFT method. For systems A and B, their 16*e* complex MN_{A-B} can form η^2-H_2 intermediates $MN_{A-B}-H_2$ along path 1 to activate dihydrogen. Although in acidic conditions (TfOH as acid) the H−H cleavage step proceeds with difficulty, molecules or ions with stronger basicity are likely to facilitate this step. For C−F, path 1 has a higher barrier and is not favorable because of the absence of η^2-H_2 intermediates $MN_{C-F}-H_2$. However, the acid molecule makes HH very favorable. A group of 16*e* TM complexes (MN_{C-F}) with delocalized π-bonds cannot activate H_2, because the strong π-bond is hard to break to provide a vacant d-orbital of TM for accepting H_2 coordination. On the other hand, 16*e* TM complexes (MN_{A-B} and INT_{A-F}) with a localized M−N π-bond can interact with H_2 to form η^2-H_2 intermediates because of the easy breaking of the localized π-bond. The coordination of H_2 with MN complexes implies MN_A and MN_B have better affinity to H_2 than MN_{C-F}; as a result, A and B could activate H_2 in mild conditions. Thus H_2 coordination is essential for the H_2 hydrogenation. The results from this study explain well the intrinsic difference among late TM catalysts for the preference of H_2 as a hydrogen source in the hydrogenation of ketones. We anticipate that the result is applicable to other H_2 hydrogenation processes catalyzed by TM complexes, providing insights in illustrating their reaction mechanisms.

Acknowledgment. This work was in part supported by Beijing Nova Fund (2005B17) and the National Natural Science Foundation of China (Grant 20703003). M.L. thanks Prof. Keiji Morokuma and Dr. Djamaladdin G. Musaev at Emory University for helpful discussions and carefully going through the manuscript. M.L. also acknowledges an Emerson Center Visiting Fellowship.

Supporting Information Available: Imaginary frequencies of transition states and optimized geometries of all stationary points along reaction pathways. This material is available free of charge via the Internet at http://pubs.acs.org.